

Dimension-Dependent Stimulated Radiative Interaction of a Single Electron Quantum Wavepacket

Avraham Gover, Yiming Pan

Department of Electrical Engineering Physical Electronics,

Tel Aviv University, Ramat Aviv 69978, ISRAEL

Abstract

In the foundation of quantum mechanics the spatial dimensions of a wavepacket are understood only in terms of an expectation value – the probability distribution of the particle location. One can still inquire, how the wavepacket size affects a physical process. Here we address the fundamental physics problem of particle-wave duality and the measurability of a free electron quantum wavepacket. Our analysis of stimulated radiative interaction of an electron wavepacket, accompanied by numerical computations, reveals two limits. In the quantum regime of long wavepacket size relative to radiation wavelength, one obtains only quantum-recoil multiphoton sidebands in the electron energy spectrum. In the opposite regime, the wavepacket interaction approaches the limit of classical point-particle acceleration. The wavepacket features can be revealed in experiments carried out in the intermediate regime of wavepacket size commensurate with the radiation wavelength.

When interacting with a radiation wave under the influence of an external force, free electrons can emit radiation spontaneously, or be stimulated to emit/absorb radiation and get decelerated/accelerated. Such an interaction can also be facilitated without an external force when the electron passes through polarizable medium. Numerous spontaneous radiative emission schemes of both kinds are well known: Synchrotron radiation, Undulator radiation, Compton Scattering, Cerenkov radiation, Smith-Purcell radiation, transition radiation [1-6]. Some of these schemes were demonstrated to operate as coherent stimulated radiative emission sources, such as Free Electron Lasers (FEL) [7-9], as well as accelerating (stimulated absorption) devices, such as Dielectric Laser Accelerator (Inverse Smith-Purcell effect) [10-12].

All of these spontaneous and stimulated radiation schemes have been analyzed in the classical limit - where they are modeled as point particles, and in the quantum limit - where they are normally modeled as plane waves [13-16]. Semi-classical wavepacket analysis of Kapitza-Dirac scattering was presented in [17]. However, a comprehensive quantum analysis of stimulated radiative interaction of a free electron wavepacket (radiative emission/absorption or equivalently acceleration/deceleration) in a finite interaction length is not available yet. It is required for bridging the classical “point particle” theory of accelerators and free electron radiators (FEL, DLA) and the quantum plane-wave limit theories of such devices, as well as related important effects as multiphoton emission/absorption quantum-recoil spectrum in the interaction of electrons with near-field radiation (PINEM) [18-22].

The interpretation and the essence of the electron quantum wavepacket and its electromagnetic interactions have been a subject of debate since the early conception of quantum mechanics. Modern QED theory and experiments indicate that spontaneous emission by a free electron is independent of its wavepacket dimensions [23-30]. However, in the present paper we focus on the stimulated emission process, and show that in this case the wavepacket dimensions do affect the interaction in a certain range of operation that we define.

In the following we solve for the stimulated radiative interaction of a single-electron wavepacket of arbitrary size, establishing first the consistency of our analysis with previous theory and experimental measurements of PINEM, FEL and DLA. We then present the main result: derivation of a new “phase-dependent” stimulated radiative interaction regime of an electron wavepacket that exhibits the physical significance of the wavepacket size and the history of its generation and transport to the interaction region. We demonstrate then how the quantum wavepacket theory transits to the classical point-particle interaction limit in this regime.

FIRST ORDER PERTURBATION ANALYSIS Our one-dimensional interaction model is based on the first order perturbation solution of the relativistic “modified Schrödinger equation” [13](see Supplementary Material 1):

$$i\hbar \frac{\partial \psi(z, t)}{\partial t} = (H_0 + H_I(t)) \psi(z, t), \quad (1)$$

where $H_0 = \varepsilon_0 + v_0(-i\hbar\nabla - \mathbf{p}_0) + \frac{1}{2\gamma_0^3 m}(-i\hbar\nabla - \mathbf{p}_0)^2$ is the free space Hamiltonian,

$m^* = \gamma_0^3 m$, and the interaction part is:

$$H_I(t) = -\frac{e\hbar}{2\gamma_0 m \omega} \left\{ e^{-i(\omega t + \phi_0)} \tilde{\mathbf{E}}(z) \cdot \nabla - e^{i(\omega t + \phi_0)} \tilde{\mathbf{E}}^*(z) \cdot \nabla \right\}, \quad (2)$$

This model is fitting for discription of the variety of interaction schemes mentioned, where $\tilde{\mathbf{E}}(z) = E_0 e^{iq_z z} \hat{\mathbf{e}}_z$ represents the dominant component of the radiation wave. We exemplify our modeling here for a case of Smith-Purcell radiation (see Fig. 1), for which the radiation wave is a Floquent mode: $\tilde{\mathbf{E}}(z) = \sum_m \tilde{\mathbf{E}}_m e^{iq_{zm} z}$ with $q_{zm} = q_{z0} + m2\pi/\lambda_G$, λ_G is the grating period, $q_{z0} = q \cos \Theta$, $q = \omega/c$ and Θ is the incidence angle of the radiation wave relative to the axial interaction dimension. The radiation wave number $q_z = q_{zm}$ represents one of the space harmonics m that satisfies synchronizm condition with the

electron [6]: $v_0 \cong \omega/q_{zm}$. We note that the analysis would be similar for the Cerenkov interaction scheme with $q_z = n(\omega)\cos\Theta$, and $n(\omega)$ the index of refraction of the medium. Furthermore, the analysis can be extended to the case of FEL and other interaction schemes [13].

The solution of Schrodinger equation to zero order (i.e. free-space propagation) is well known. Assuming that the initial wavepacket, which is emitted at some point $z = -L_D$ near the cathode face (or any other electron source) at time $t = -t_D$, is a gaussian at its waist, then:

$$\psi^{(0)}(z, t) = \left(2\pi\sigma_{p_0}^2\right)^{-\frac{1}{4}} \int \frac{dp}{\sqrt{2\pi\hbar}} \exp\left(-\frac{(p-p_0)^2}{4\sigma_{p_0}^2}\right) e^{ip(z+L_D)/\hbar} e^{-iE_p(t+t_D)/\hbar} = \int \frac{dp}{\sqrt{2\pi\hbar}} c_p^{(0)} e^{-iE_p t/\hbar} |p\rangle, \quad (3)$$

where $|p\rangle = e^{ipz/\hbar}$. Note that $L_D, t_D = L_D/v_0$ are the “effective” drift length and drift time of the wavepacket center, that are somewhat different from the geometric distance and drift time from the cathode physical face. Expanding the energy dispersion relation to second order $E_p = c\sqrt{m^2c^2 + p^2} \approx E_0 + v_0(p - p_0) + \frac{(p - p_0)^2}{2m^*}$, the wavepacket development in momentum space is then given by

$$c_p^{(0)} = \left(2\pi\sigma_{p_0}^2\right)^{-\frac{1}{4}} \exp\left(-\frac{(p - p_0)^2}{4\tilde{\sigma}_p^2(t_D)}\right) e^{i(p_0 L_D - E_0 t_D)/\hbar}, \quad (4)$$

with $\tilde{\sigma}_p^2(t_D) = \sigma_{p_0}^2 \left(1 + i t_D/t_{R_\parallel}\right)^{-1}$, $\sigma_{p_0} = \hbar/2\sigma_{z_0}$, $t_{R_\parallel} = \frac{m^*\hbar}{2\sigma_{p_0}^2} = 4\pi \frac{\sigma_{z_0}^2}{\lambda_c^* c}$, and we defined $\lambda_c^* = \lambda_c/\gamma^3$ with $\lambda_c = h/mc$ – the Compton wavelength.

We now solve Eq.1 using the first order perturbation theory in momentum space (see Supplementary Material 2)

$$\psi(z, t) = \psi^{(0)}(z, t) + \psi^{(1)}(z, t) = \int \frac{dp}{\sqrt{2\pi\hbar}} \left(c_p^{(0)} + c_p^{(1)}\right) e^{-iE_p t/\hbar} |p\rangle. \quad (5)$$

and then calculate the electron momentum density distribution after interaction:

$$\begin{aligned}\rho(p') &= \rho^{(0)}(p') + \rho^{(1)}(p') + \rho^{(2)}(p') \\ &= \frac{|c^{(0)}(p')|^2 + 2\text{Re}\{c^{(1)*}(p')c^{(0)}(p')\} + |c^{(1)}(p')|^2}{\int dp'(|c^{(0)}(p')|^2 + |c^{(1)}(p')|^2)},\end{aligned}\quad (6)$$

Where

$$\rho^{(0)}(p') = |c^{(0)}(p')|^2 = (2\pi\sigma_{p_0}^2)^{-\frac{1}{2}} \exp\left(-\frac{(p' - p_0)^2}{2\sigma_{p_0}^2}\right) \quad (7)$$

is the initial Gaussian momentum density distribution.

PHASE-INDEPENDENT MOMENTUM DISTRIBUTION – FEL GAIN. First we draw attention to the second order density distribution (third term in Eq.6);

$$\begin{aligned}\rho^{(2)}(p') &= \Upsilon^2 \left[\left(\frac{p' + p_{rec}^e}{p_0} \right)^2 \rho^{(0)}(p' + p_{rec}^e) - \rho^{(0)}(p') \right] \text{sinc}^2\left(\frac{\bar{\theta}_e}{2}\right) \\ &\quad + \Upsilon^2 \left[\left(\frac{p' - p_{rec}^a}{p_0} \right)^2 \rho^{(0)}(p' - p_{rec}^a) - \rho^{(0)}(p') \right] \text{sinc}^2\left(\frac{\bar{\theta}_a}{2}\right).\end{aligned}\quad (8)$$

where the two terms in $\rho^{(2)}$ display two sidebands proportional to the initial density distribution $\rho^{(0)}$ shifted centrally to $p_0 \mp p_{rec}^{(e,a)}$ due to photon emission and absorption recoils (see Fig.2). Its first order moment results in the momentum acceleration/deceleration associated with stimulated radiative interaction:

$$\Delta p^{(2)} = \int \rho^{(2)}(p') p' dp' = \Upsilon^2 \left(\frac{\hbar\omega}{v_0} \right) \left[\text{sinc}^2\left(\frac{\bar{\theta}_e}{2}\right) - \text{sinc}^2\left(\frac{\bar{\theta}_a}{2}\right) \right]. \quad (9)$$

where $\Upsilon = \frac{eE_0 L_I}{4\hbar\omega}$, $\bar{\theta}_{e,a} = \bar{\theta} \pm \frac{\varepsilon}{2}$, and $\bar{\theta} = \left(\frac{\omega}{\nu_0} - q_z \right) L_I$ is the classical “interaction detuning parameter” [9], and $\varepsilon = \delta \left(\frac{\omega}{\nu_0} \right) L_I = 2\pi\delta L_I / \beta_0 \lambda$ is the interaction–length quantum recoil parameter [13] and $\delta = \hbar\omega / 2m^* \nu_0^2 \ll 1$. Remarkably Eq.7 is independent of the wavepacket distribution $\rho^{(0)}$, and is satisfactorily consistent with the stimulated emission/absorption terms in the quantum-electrodynamic photon emission rate expression dv_q / dt , that was derived in [13] for a single plane-wave electron wavefunction in the limit $\rho^{(0)}(p') = \delta(p - p')$:

$$\frac{dv_q}{dt} = \Gamma_{sp} \gamma_0 \nu_0 \left[\left(\nu_q + 1 \right) \frac{1}{\gamma_e \nu_e} \text{sinc}^2 \left(\frac{\bar{\theta}_e}{2} \right) - \nu_q \frac{1}{\gamma_e \nu_e} \text{sinc}^2 \left(\frac{\bar{\theta}_a}{2} \right) \right]. \quad (10)$$

Using Eq. 9-10 in the conservation of energy and momentum relation,

$$\Delta p^{(2)} = - \frac{L_I}{\nu_0} \left(\frac{\hbar\omega}{\nu_0} \right) \left(\frac{dv_q}{dt} \right)_{st}, \quad (11)$$

We can relate the interaction parameter Υ to the spontaneous radiation emission coefficient Γ_{sp}

$$\Upsilon^2 = \frac{L_I}{\nu_0} \Gamma_{sp} \nu_q, \quad (12)$$

and derive an explicit expression for the spontaneous emission rate per mode Γ_{sp} from the relation between ν_q and $|E_0|^2$. It is also interesting to point out that in the limit of negligible recoil relative to the finite-length homogeneous line broadening:

$$\varepsilon = \pi \frac{\hbar\omega}{m^* \nu_0^2} \frac{L_I}{\beta_0 \lambda} \ll 1, \quad (13)$$

$$\Delta p^{(2)} = \frac{\hbar\omega}{v_0} \Upsilon^2 \varepsilon \frac{d}{d\theta} \text{sinc}^2(\bar{\theta}/2), \quad (14)$$

consistently with the conventional classical gain expression of Smith-Purcell and Cerenkov FELs, as well as other FELs[9,13]. In particular it is instructive to note that the coefficient $\Upsilon^2 \varepsilon$ scales like L^3 . This suggests that similarly to classical “point-particle” FEL theory also the second order acceleration/gain of a quantum wavepacket involves a process of bunching on the level of the single electron quantum wave.

It should be noted that second order (in the field) acceleration/deceleration (Eq. 9) is only possible out of synchronism ($\bar{\theta} \neq 0$) and is due to the asymmetry of emission and absorption recoils in the interaction length. Net acceleration/deceleration (gain/loss) is possible in the FEL quantum limit $\varepsilon \gg 1$ (opposite of Eq.13) in which the homogeneously broadened emission/absorption lines do not overlap (Eq.9-10). In the more common case of classical FEL gain (Eq.14): $\bar{\theta}_e \simeq \bar{\theta}_a \simeq \bar{\theta}$, gain/attenuation are possible only if the degeneracy of emission/absorption is lifted by operating out of synchronism ($\bar{\theta} \neq 0, \sim \pi$).

In PINEM, the near field interaction takes place along a very short interaction length relative to the wavelength. Our analysis reduces to this case when $\bar{\theta} = 2\pi L_I / \beta_0 \lambda \ll \pi$ (see Supp. Eq. 30). Then the emission and absorption lines are degenerate and there is no net-gain. However, the emission and absorption lines in the momentum distribution function (Eq.8 with $\bar{\theta}_e = \bar{\theta}_a \simeq 0$) are still separable then if the quantum recoil momentum $p_{\text{rec}}^{(0)}$ is significant relative to the wavepacket momentum spread

$$p_{\text{rec}}^{(0)} = \frac{\hbar\omega}{v_0} \gg \sigma_{p0}, \quad (15)$$

In this limit the distribution shows distinct symmetric sidebands, spaced by $p_{\text{rec}}^{(0)}$ on both sides of the center initial momentum p_0 as displayed in Fig. 2. Similar sideband development is shown in supplementary video 1 based on numerical solution of Eq. 1

for weak interaction $\Upsilon < 1$. This result is similar to the measured spectrum in PINEM experiments [18-22], where multiple ($\gg 3$) sidebands were observed due to multiple photon emission/absorption. In our example of weak interaction only two emission/absorption sidebands are observed.

PHASE-DEPENDENT MOMENTUM DISTRIBUTION The second order perturbation term lost the dependence on the phase ϕ_0 of the wavepacket center relative to the laser field, and therefore does not reveal any specific features of the single electron wavepacket. We now draw attention to the phase-dependent density distribution (see Supplementary Eq.31). This term has not been considered in previous analyses, but in the present work it is of prime interest because it retains the dependence on the phase ϕ_0 . In the limit of negligible recoil $\varepsilon = 0$ and to first order in $p_{\text{rec}}^{(0)}$, one obtains from first order expansion in terms of δ :

$$\rho^{(1)}(p') = 4 \left(\frac{\hbar \omega / v_0}{p_0} \right) \Upsilon \rho^{(0)}(p') \text{sinc} \left(\frac{\bar{\theta}}{2} \right) e^{-\Gamma^2/2} \cos \left(\frac{\bar{\theta}}{2} + \phi_0 + \varphi \right) \left[1 + \frac{\Gamma^2 p'}{2m^* v_0} - \frac{(p' - p_0) p'}{2\sigma_{p_0}^2} \right]. \quad (16)$$

where

$$\begin{aligned} \Gamma &= \frac{\omega}{v_0} \sigma_z(t_D) = \frac{2\pi \sigma_z(t_D)}{\beta \lambda}, \\ \varphi &= \frac{2\omega t_D}{mv_0} (p' - p_0). \end{aligned} \quad (17)$$

The coefficient $e^{-\Gamma^2/2}$ assures that the first order term of the momentum distribution $\rho^{(1)}$ is diminished when $\Gamma \gg 1$, namely when the wavepacket expands on its way from the source beyond the size of the interaction wavelength. Neglecting φ , the momentum transfer is:

$$\Delta p^{(1)} = \int \rho^{(1)}(p') p' dp' = \frac{\Gamma^2 e^{-\Gamma^2/2}}{2\gamma_0^2} \frac{eE_0 L_I}{v_0} \text{sinc} \left(\frac{\bar{\theta}}{2} \right) \cos \left(\phi_0 + \frac{\bar{\theta}}{2} \right), \quad (18)$$

for $\Upsilon \ll 1$. This expression can be contrasted with the classical “point particle” momentum transfer equation

$$\Delta p_{point} = \frac{eE_0 L_I}{v_0} \text{sinc}\left(\frac{\bar{\theta}}{2}\right) \cos\left(\phi_0 + \frac{\bar{\theta}}{2}\right).$$

and the corresponding expression for stimulated-superradiant emission energy $W_q = v_0 \Delta p_{point}$ [31]. Except for the reduction factor:

$$\Delta p^{(1)} / \Delta p_{point} = \Gamma^2 e^{-\Gamma^2/2} / 2\gamma_0^2, \quad (19)$$

the acceleration/deceleration of the quantum wavepacket (Eq.18) scales with $\bar{\theta}$ and ϕ_0 similarly to the case of a point particle.

Figures 3 and 4 display the momentum density distribution $\rho^{(0)} + \rho^{(1)}$ for the case $\bar{\theta} = 0$ and acceleration phase: $\phi_0 = 0$. In this explicitly quantum limit of wavepacket acceleration the resultant post-interaction distribution $\rho(p') = \rho^{(0)} + \rho^{(1)} + \rho^{(2)}$ does not change much in width, but it gets lopsided towards positive momentum. The peak distribution is shifted about $\Delta p^{(1)} = \frac{2}{\gamma_0^2} \frac{\hbar \omega}{v_0} \Upsilon$ for $\Gamma = \sqrt{2}$. A left shifted momentum distribution would appear in the case of deceleration for phase $\phi_0 = \pi$. These low-gain phase dependent acceleration/deceleration features are confirmed qualitatively by the numerical simulations (Supplementary Material video-2(a,b)).

THE WAVE-PARTICLE TRANSITION. The wavepacket-size scaling of the first order perturbation expression (19) is well expected in the long wavepacket limit $\Gamma(L_D) = 2\pi\sigma_z(L_D)/\beta\lambda \gg 1$. In this quantum limit the quantum wavepacket behaves as a plane wave and no phase-dependent synchronous wave acceleration is possible, and therefore $\Delta p^{(1)}/\Delta p_{point}$ diminishes exponentially. However, the scaling down to zero of this expression in the short wavepacket limit $\Gamma(L_D) = 2\pi\sigma_z(L_D)/\beta\lambda \ll 1$ does not result in the expected point-particle acceleration limit $\Delta p_{pack}/\Delta p_{point} \rightarrow 1$. This

discrepancy may be an indication of the limitation of first order perturbation analysis, failing to reduce to the classical limit in the range $\Upsilon \ll 1$.

In order to study the wave-particle transition regime we resorted to numerical solution of Eq. 1 for different values of Υ . Video 3a,b display phase-dependent linear acceleration/deceleration in the wavepacket parameters regime of wave/particle transition: $\theta = 0, \theta_a = 0, \Gamma = 0.2, \Upsilon = 1.5$. In this example the wavepacket accelerates almost as a point particle. Comparison of Videos 2 and 3 indicates near proportionality relation of the net acceleration with Υ (or E_0). In Fig. 5 we show the computed dependence of $\Delta p_{pack}/\Delta p_{point}$ on $\Gamma(L_D)$ in the transition range $0.2 < \Gamma < 3$. The two computed examples of $\Upsilon = 0.4, 1.6$ follow quite accurately a Gaussian fitting curve $\exp(-\Gamma^2/2)$, that decays for $\Gamma \gg 1$, and approaches the limit $\Delta p_{pack}/\Delta p_{point} \rightarrow 1$ for $\Gamma \ll 1$, as expected. For comparison we show also the first-order perturbation curve (19). Good match to the Gaussian function was found in all simulation expamples for which $\Upsilon < \sim 1$.

Remarkably, all examples of numerical computations in this regime fitted the Gaussian dependence on the variable $\Gamma(L_D) = 2\pi\sigma_z(t_D)/\beta\lambda$ - meaning that the relevant wavepacket parameter is the history-dependent spatial size of the wavepacket upon entrance to the interaction region after any drift time t_D , independently of the initial wavepacket size σ_{z0} . However, since σ_{z0} determines the wavepacket width in momentum space - $\sigma_{p0} = \hbar/2\sigma_{z0}$, the momentum acceleration resolution in the small photon exchange range $\Upsilon < \sim 1$ is marginal:

$$\left| \frac{\Delta p_{pack}}{\sigma_{p0}} < \frac{\Delta p_{point}}{\sigma_{p0}} = 8\pi\gamma_0 \frac{\sigma_{z0}}{\lambda\beta} \right. \quad (20)$$

An important observation can be made now from inspection of the expression for the wavepacket expansion in free drift:

$$\sigma_z(t_D) = \sqrt{\sigma_{z0}^2 + \left(\frac{\lambda_c^*}{4\pi} \frac{ct_D}{\sigma_{z0}} \right)^2}, \quad (21)$$

It is obvious that $\sigma_{z0} \rightarrow 0$ is not the point particle limit, since then the wavepacket size explodes. Moreover, $\sigma_z(t_D)$ cannot be arbitrarily small, for any given t_D , (or $L_D = v_0 t_D$) it has an absolute minimum:

$$\sigma_z(t_D)|_{\min} = \sqrt{\frac{\lambda_c^*}{2\pi} ct_D}, \quad (22)$$

This corresponds to a minimum value of Γ for fixed frequency ω

$$\Gamma_{\min} = \frac{\omega}{v_0} \sqrt{\frac{\lambda_c^*}{2\pi} ct_D}, \quad (23)$$

which means that for fixed drift length L_D the curve in Fig. 5 has physical meaning only for $\Gamma > \Gamma_{\min}$.

We define a critical drift length $z_G = v_0 t_D$ as the distance for which $\Gamma_{\min} = \sqrt{2}$, that corresponds to the point where $\Delta p_{\text{pack}}/\Delta p_{\text{point}} = 1/e$:

$$z_G = \frac{\beta_0^3 \gamma_0^3}{\pi} \frac{\lambda^2}{\lambda_c}, \quad (24)$$

We come to the significant observation that for drift distances away from the source $L_D \gg z_G$, wavepacket-dependent linear (in the field) acceleration/deceleration of a single electron is always diminished, because the wavepacket inevitably spreads wider than the interacting wavelength, and the phase ϕ_0 of the electron wavepacket center relative to the wave at the interaction region becomes undefined. This observation is also consistent with an earlier suggestion that the quantum wavepacket spread poses a fundamental physical high frequency or short wavelength limit $\lambda_{\text{cutoff}} = (\pi \lambda_c / \beta^3 \gamma^3)^{1/2}$ on measurement of particle beam shot-noise, challenging the conventional mathematical “point-particle” model presentation of shot-noise as an unbound “white noise” [32].

WAVEPACKET-DEPENDENT STIMULATED INTERACTION MEASUREMENT The phase-dependent linear field acceleration regime of a wavepacket $(\rho^{(l)}, \Delta p^{(l)})$ is of fundamental interest, because contrary to the phase-independent acceleration $(\rho^{(2)}, \Delta p^{(2)})$, its characteristics depend on the quantum wavepacket dimensions, and at the same time respond to the classical phase of the wave. So far, previous laser acceleration experiments of single electrons [10-12,18] were carried out only in the second order acceleration regime, where only broadening of the momentum spectrum is observable at synchronism, without net acceleration.

We point out that the effect of the wavepacket size on the acceleration of a single electron wavepacket can be measured in the phase-dependent weak interaction limit if one varies the parameter $\Gamma = 2\pi\sigma_z(t_D)/\beta_0\lambda$ over a range near $\Gamma \leq \sqrt{2}$, and measures a dependence of the wavepacket acceleration as in Fig. 5 and a dependence on the laser phase ϕ_0 as in Eq.18. Experimentally one can scan over $\Gamma(t_D)$, $\sigma_z(t_D)$ by performing the radiative interaction at different drift distances $L_D = v_0 t_D$, as long as one keeps $L_D < z_G(\lambda, \beta_0)$. Also it may be possible to vary λ, β_0 , and interact repeatedly with the same electron.

A measurement of acceleration at different distances and wavelengths is analogous to measurement of the transverse diffraction characteristics of a laser beam of wavelength λ by measuring its transmission through apertures of radius R at different distances L from the beam waist. Such measurements reveal information about the beam, if made at distances shorter than or commensurate with the aperture Rayleigh length $z_R = \pi R^2 / \lambda$. At distances $z > z_R$ the transmitted beam would always be attenuated, independently of the initial waist size, while for $z < z_R$ the transmission through the aperture depends on the spot size at the aperture. In the stimulated emission experiments the radiation interaction wavelength $\beta_0\lambda$ acts as a moving

longitudinal aperture (analogous to the diffraction aperture R) with the longitudinal Compton wavelength λ_c^* / β playing the same role as the optical wavelength λ in the diffraction experiment.

CONCLUSIONS. Here we related to the fundamental questions of the physical significance of a single particle quantum wavepacket and the wave to particle transition in the classical electrodynamics limit. The presented semiclassical first order perturbation analysis and the numerical computations show that stimulated interaction of a single electron wavepacket with radiation can be dependent on the features of the wavepacket, its history and its spatial position relative to the phase of the accelerating wave. This can only happen in a certain range, close enough to the electron emission source under the condition of small quanta exchange. This was not observed so-far in previous experiments of PINEM (in the quantum-recoil-dominated regime), and DLA (in the classical negligible-quantum-recoil regime) that operated out of this range of wavepacket phase-dependent, and therefore could display only symmetric momentum broadening of the interacting electrons, without net acceleration.

On passing, we also showed that the phase-independent, second order (in the field) acceleration solution of stimulated radiative interaction of an electron wavepacket is consistent with the quantum and classical multi-particle theory limits of DLA and FEL.

ACKNOWLEDGEMENTS We acknowledge Yakir Aharonov, A. Friedman, S. Rushin and Amnon Yariv for useful discussions and comments. The work was supported in parts by DIP (German-Israeli Project Cooperation) and US-Israel Binational Science Foundation, and by the PBC program of the Israel council of higher education. Correspondance and requests for materials should be addressed to A. G. (gover@eng.tau.ac.il) and Y.P. (yimingpan@mail.tau.ac.il).

REFERENCES

1. Brau, Charles A. Modern Problems in Classical Electrodynamics. *Oxford University Press*, ISBN 0-19-514665-4 (2004).
2. H. Motz, *J. Appl. Phys.* **22**, 527-535 (1951).
3. V. P. Sukhattmee, P. W. Wolff, *J. Appl. Phys.*, **44**, 2331-2334 (1973).
4. Cherenkov, P. A., *Doklady Akademii Nauk SSSR*. **2**, 451(1934).
5. V. L. Ginzburg and I. M. Frank, *Zh. Eksp. Teor. Fiz.* **16**, 15–22 (1946).
6. S. J. Smith and E. M. Purcell, *Phys. Rev.* **92**, 1069 (1953).
7. J. M. Madey, *Appl. Phys.* **42**, 1906-1913 (1971).
8. Pellegrini, C., A. Marinelli, and S. Reiche. *Reviews of Modern Physics* **88(1)**, 015006 (2016).
9. Gover, A., and P. Sprangle, *IEEE Journal of Quantum Electronics* **17(7)**, 1196-1215 (1981).
10. Peralta, et al., *Nature* **503(7474)**, 91-94 (2013).
11. Breuer, J. and Hommelhoff, P. *Phys. Rev. Lett.* **111(13)**, 134803 (2013).
12. McNeur, J., Kozak, M., Ehberger, D., Schönenberger, N., Tafel, A., Li, A. and Hommelhoff, P. *Journal of Physics B: Atomic, Molecular and Optical Physics*, **49(3)**, 034006 (2016).
13. Friedman, A., Gover, A., Kurizki, G., Ruschin, S., & Yariv, A., *Reviews of Modern Physics* **60(2)**, 471 (1988).
14. Peter Kling et al., *New J. Phys.* **17**, 123019 (2015).
15. I. Kaminer, et al., *Phys. Rev. X* **6**, 011006 (2016).
16. Ivanov, I. P. *Phys. Rev. A* **93**, 053825 (2016).
17. Efremov, M. A., and M. V. Fedorov. *Journal of Physics B: Atomic, Molecular and Optical Physics* **33.20** (2000): 4535.
18. Feist, A. et al. *Nature* **521**, 200-203 (2015).
19. Herink, G., Solli, D. R., Gulde, M., & Ropers, C. *Nature*, **483(7388)**, 190-193 (2012).
20. Barwick, B.; Flannigan, D. J.; Zewail, A. H. *Nature* **462**, 902–906(2009).

21. García de Abajo, F. Javier, Ana Asenjo-Garcia, and Mathieu Kociak. "Multiphoton absorption and emission by interaction of swift electrons with evanescent light fields." *Nano Letters* **10.5** (2010): 1859-1863.
22. Piazza, L. U. C. A., Lummen, T. T. A., Quinonez, E., Murooka, Y., Reed, B. W., Barwick, B., & Carbone, F. *Nature Communications*, 6(2015).
23. P. Krekora, R. E. Wagner, Q. Su, and R. Grobe, *Laser Phys.* **12**, 455 (2002).
24. E. A. Chowdhury, I. Ghebregziabiher, and B. C. Walker, *J. Phys. B* **38**, 517 (2005).
25. J. Peatross, J. P. Corson, and G. Tarbox, *Am. J. Phys.* **81**, 351 (2013).
26. A. Barut, *Found. Phys. Lett.* **1**, 47 (1988).
27. Ware, Michael, et al. *Optics letters* **41(4)**, 689-692 (2016).
28. Peatross, Justin, et al. *Phys. Rev. Lett.* **100**, 153601 (2008).
29. Corson, J.P., Peatross, J., Müller, C. and Hatsagortsyan, K.Z. *Physical Review A*, 84(5), 053831 (2011).
30. P. M. Anisimov, TUP006 Proceedings of FEL2015, Daejeon, Korea.
31. Gover, A., *Physical Review Special Topics-Accelerators and Beams*, **8(3)**, 030701(2005).
32. R. Iancu, A. Gover, A. Nause, TUP007 Proceedings of FEL, Basel, Switzerland (2014).

FIGURES

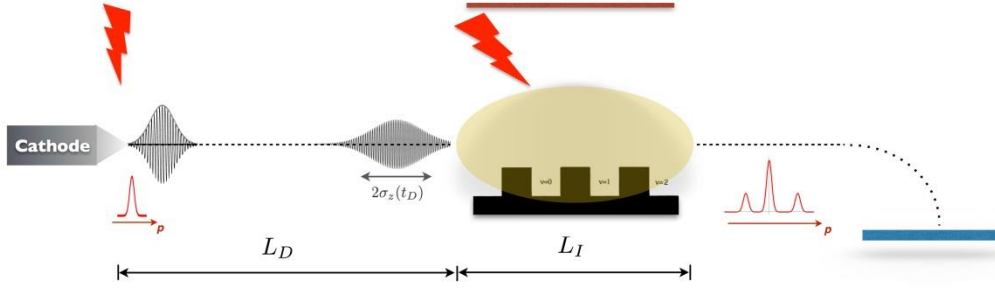


Fig. 1: The experiment setup. Single electron wavepackets are photo-emitted from a cathode driven by a fs laser. After a free propagation length L_D , the expanded wavepacket passes next to the surface of a grating, and interacts with the near-field radiation, that is excited by an IR wavelength laser, phase locked to the photo-emitting laser. The momentum distribution of the modulated wavepacket is measured with an electron energy spectrometer.

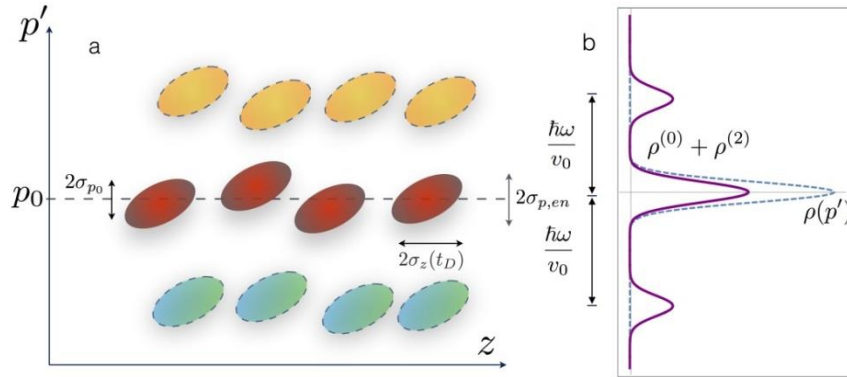


Fig. 2: The quantum recoil limit of electron-laser interaction. The phase-space distribution of an ensemble of quantum wavepackets after interaction with the near-field is shown in (a), and its final momentum distribution is shown in (b). In this limit the condition $p_{rec} = \frac{\hbar\omega}{v_0} \gg \sigma_{en} > \sigma_{p0}$ is satisfied, where σ_{en} is the ensemble momentum spread.

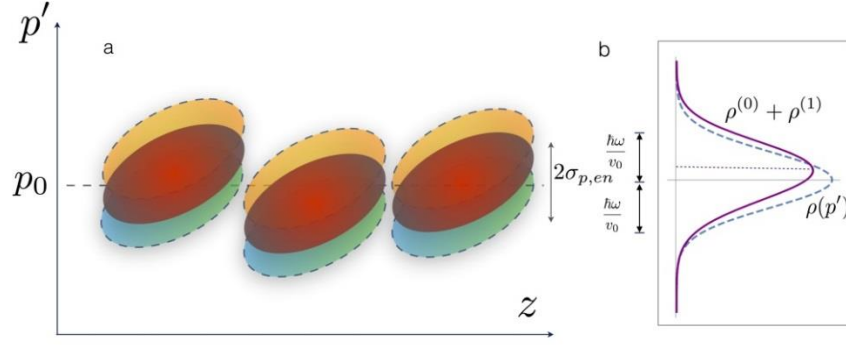


Fig. 3: Linear field acceleration of a phase-defined wavepacket. The phase space distribution of electron quantum wavepackets interacting weakly with the near-field wave is shown in (a), and its final momentum distribution in (b). In this limit

$$\Gamma = \frac{2\pi\sigma_z(t_D)}{\beta\lambda} \simeq 1 \text{ and } p_{rec} = \frac{\hbar\omega}{v_0} \ll \sigma_{p0}.$$

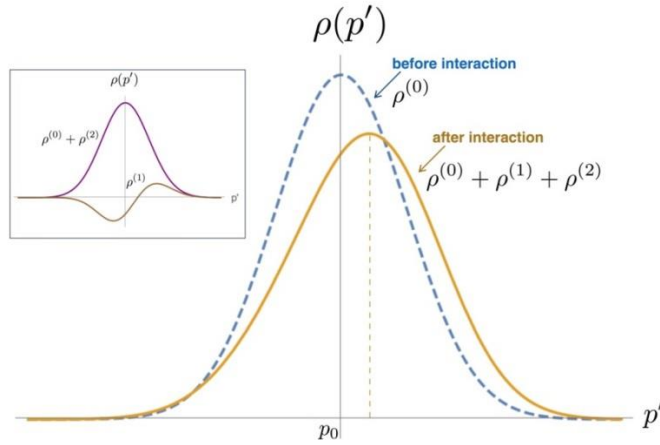


Fig. 4: Total final momentum distribution of a Linear field accelerated phase-defined wavepacket. The parameters are for maximal momentum gain: $\bar{\theta} = 0$ (velocity synchronism), $\phi_0 = 0$ (accelerating phase), $\Gamma = \sqrt{2}$. The inset shows the incremental distributions $\rho^{(1)}$ and $\rho^{(0)} + \rho^{(2)}$ separately.

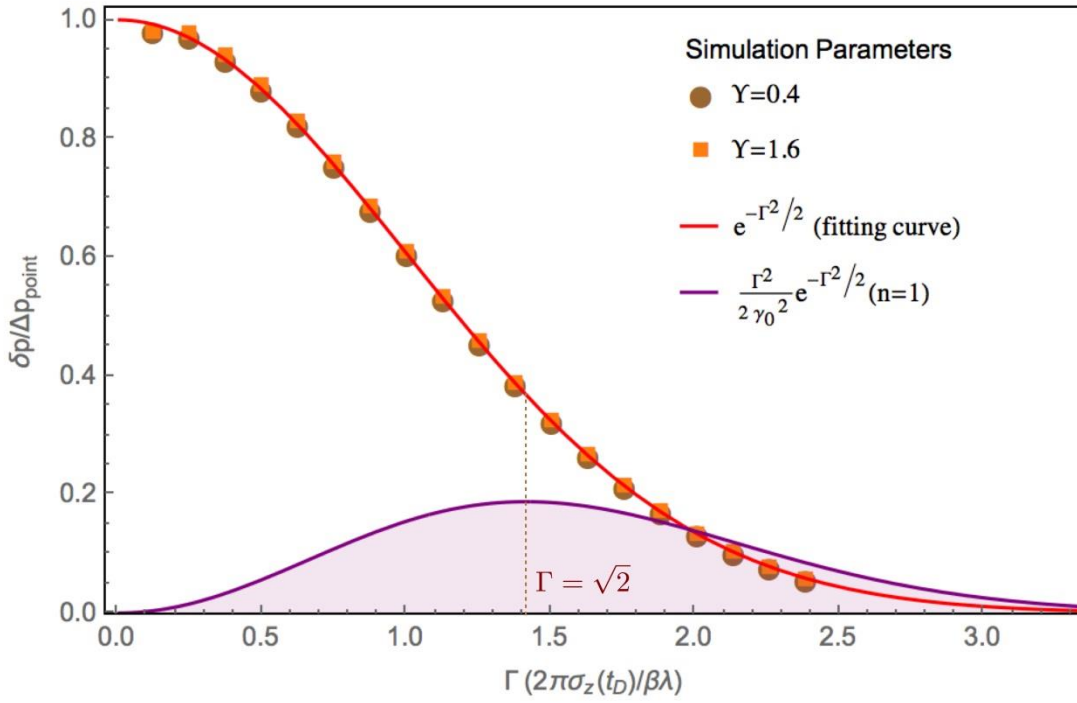


Fig. 5: The reduction factor of wavepacket acceleration/deceleration relative to the “point-particle” classical case, as calculated from numerical solution of Schrodinger equation (red fitting curve), and compared to the first-order perturbation expression (21) (violet). The numerical computation with parameters $\beta_0 = 0.7, \gamma_0 = 1.4, \beta_0 \lambda = \Lambda_G = 2 \mu m, L_l = 8 \mu m$ reproduces the short (point-particle) limit $\delta p / \Delta p_{\text{point}} \rightarrow 1$ when $\Gamma \ll 1$.

Supplementary Materials:

Stimulated Radiation Interaction of a Single Electron Quantum Wavepacket

Avraham Gover, Yiming Pan

*Department of Electrical Engineering Physical Electronics,
Tel Aviv University, Ramat Aviv 69978, ISRAEL*

1. The modified ‘relativistic’ Schrodinger equation from the Klein-Gordon equation

To describe the Klein-Gordon equation, let’s start with the relativistic energy-momentum dispersion

$$E_p^2 = p^2 c^2 + m^2 c^4, \quad (1)$$

where m is electron rest mass and c the speed of light. To obtain the KG equation, we replace $E \rightarrow i\hbar \frac{\partial}{\partial t}$, $\mathbf{p} \rightarrow -i\hbar \nabla - e\mathbf{A}$ (minimal coupling with electromagnetic radiation) and apply the differential operator on a wavefunction:

$$\left(i\hbar \frac{\partial}{\partial t} \right)^2 \psi(r, t) = c^2 (-i\hbar \nabla - e\mathbf{A})^2 \psi(r, t) + m^2 c^4 \psi(r, t) \quad (2)$$

where e is an electron charge. The Klein-Gordon equation can describe the relativistic electrons with most radiation schemes considered if spin effect is negligible. If the radiation field is weak, which is the case for $e\mathbf{A} / mc \ll 1$, then it can be well approximated by a quasi-relativistic effective Schrodinger equation. The approximation is based on the assumption that the solution of $\psi(r, t)$ is a single quasiharmonic positive energy wave [Ref.13 in the main text]

$$\psi(r, t) = u(r, t) e^{-i\varepsilon_0 t / \hbar} \quad (3)$$

where $\varepsilon_0 = \sqrt{p_0^2 c^2 + m^2 c^4} = \gamma_0 m c^2$, p_0 the center momentum and the component $u(r, t)$ is a slowly varying function. Then substitution of Eq.(3) in (2) and cancelling the fast-varying phase $e^{-i\varepsilon_0 t / \hbar}$, results in

$$i\hbar \frac{\partial u(r,t)}{\partial t} = \left(\frac{c^2 (-i\hbar \nabla - e\mathbf{A})^2 + (m^2 c^4 - \varepsilon_0^2)}{2\varepsilon_0} \right) u(r,t) + \frac{\hbar^2}{2\varepsilon_0} \frac{\partial^2 u(r,t)}{\partial t^2} \quad (4)$$

This is the exact expression for the slow part function $u(r,t)$, and to the first order approximation in the time derivatives, we obtain

$$i\hbar \frac{\partial u(r,t)}{\partial t} = \left(\frac{c^2 (-i\hbar \nabla - e\mathbf{A})^2 + (m^2 c^4 - \varepsilon_0^2)}{2\varepsilon_0} \right) u(r,t)$$

Successive iterative substitution of the equation into the exact formula (4) results in now

$$i\hbar \frac{\partial u(r,t)}{\partial t} = \left(\frac{c^2 (-i\hbar \nabla - e\mathbf{A})^2 + (m^2 c^4 - \varepsilon_0^2)}{2\varepsilon_0} \right) u(r,t) - \frac{1}{2\varepsilon_0} \left(\frac{c^2 (-i\hbar \nabla - e\mathbf{A})^2 + (m^2 c^4 - \varepsilon_0^2)}{2\varepsilon_0} \right)^2 u(r,t) \quad (5)$$

Now the Klein-Gordon equation can be re-expressed in the form of the effective Schrodinger equation,

$$i\hbar \frac{\partial \psi(r,t)}{\partial t} = i\hbar \frac{\partial u(r,t)}{\partial t} e^{-i\varepsilon_0 t/\hbar} + \varepsilon_0 u(r,t) e^{-i\varepsilon_0 t/\hbar} = H\psi(r,t) \quad (6)$$

where the Hamiltonian is

$$H = \varepsilon_0 + \left(\frac{c^2 (-i\hbar \nabla - e\mathbf{A})^2 + (m^2 c^4 - \varepsilon_0^2)}{2\varepsilon_0} \right) - \frac{1}{2\varepsilon_0} \left(\frac{c^2 (-i\hbar \nabla - e\mathbf{A})^2 + (m^2 c^4 - \varepsilon_0^2)}{2\varepsilon_0} \right)^2 \quad (7)$$

The Hamiltonian can be split into an electronic unperturbed part and a radiative perturbation part $H = H_0 + H_I(t)$, where

$$H_0 \simeq \varepsilon_0 + v_0 (-i\hbar \nabla - \mathbf{p}_0) + \frac{1}{2\gamma_0^3 m} (-i\hbar \nabla - \mathbf{p}_0)^2 \quad (8)$$

and to the first order in \mathbf{A} ,

$$H_1 \approx -e\mathbf{A} \left(\frac{-i\hbar \nabla}{\gamma_0 m} \right) \quad (9)$$

where $v_0 = p_0 / \gamma_0 m$. For the case of our concern, $\mathbf{E} = -\frac{\partial \mathbf{A}}{\partial t} = \text{Re}[\tilde{\mathbf{E}}(z) e^{-i(\omega t + \phi_0)}]$, then the perturbation Hamiltonian is

$$H_1 = -\frac{e\hbar}{2\gamma_0 m \omega} \left(e^{-i(\omega t + \phi_0)} \tilde{\mathbf{E}}(z) \cdot \nabla - e^{i(\omega t + \phi_0)} \tilde{\mathbf{E}}^*(z) \cdot \nabla \right) \quad (10)$$

$$\tilde{\mathbf{E}}(z) = E_0 e^{iq_z z} \hat{\mathbf{e}}_z$$

2. The first order perturbation analysis

The equation to be solved is the ‘relativistic’ Schrodinger equation

$$i\hbar \frac{\partial \psi(z, t)}{\partial t} = (H_0 + H_1(t)) \psi(z, t), \quad (11)$$

with H_0 given by Eq.8 and H_1 given by Eq.10. We solve this equation by perturbation theory. The solution of Schrodinger equation to zero order (i.e. free space propagation) is well known. Assuming that the initial wavepacket, which is emitted at some point $z = -L_D$ near the cathode face at time $t = -t_D$, is a gaussian at its waist, then:

$$\psi^{(0)}(z, t) = \left(2\pi\sigma_{p_0}^2 \right)^{-\frac{1}{4}} \int \frac{dp}{\sqrt{2\pi\hbar}} \exp\left(-\frac{(p-p_0)^2}{4\sigma_{p_0}^2} \right) e^{ip(z+L_D)/\hbar} e^{-iE_p(t+t_D)/\hbar} = \int \frac{dp}{\sqrt{2\pi\hbar}} c_p^{(0)} e^{-iE_p t/\hbar} |p\rangle, \quad (12)$$

where $|p\rangle = e^{ipz/\hbar}$. Note that $L_D, t_D = L_D/v_0$ are the “effective” drift length and drift time of the wavepacket center, that are somewhat different from the geometric distance and drift time from the cathode face. This is because of the initial section of electron acceleration from the cathode and because the wavepacket longitudinal waist may be somewhere within the cathode.

Expanding the energy dispersion relation to second order

$$E_p = c\sqrt{m^2 c^2 + p^2} \approx E_0 + v_0(p - p_0) + \frac{(p - p_0)^2}{2m^*}, \quad (13)$$

The wavepacket development in momentum space is then given by

$$c_p^{(0)} = \left(2\pi\sigma_{p_0}^2\right)^{-\frac{1}{4}} \exp\left(-\frac{(p-p_0)^2}{4\tilde{\sigma}_p^2(t_D)}\right) e^{i(p_0 L_D - E_0 t_D)/\hbar}, \quad (14)$$

with

$$\begin{aligned} \tilde{\sigma}_p^2(t_D) &= \sigma_{p_0}^2 \left(1 + i t_D / t_{R_{\parallel}}\right)^{-1}, \\ \sigma_{p_0} &= \hbar / 2\sigma_{z_0}, \\ t_{R_{\parallel}} &= \frac{m^* \hbar}{2\sigma_{p_0}^2} = 4\pi \frac{\sigma_{z_0}^2}{\lambda_c^* c}, \end{aligned} \quad (15)$$

where we define

$$\lambda_c^* = \lambda_c / \gamma^3, \quad (16)$$

with $\lambda_c = \hbar / mc$ – the Compton wavelength. The wavepacket development in space is calculated from Equation (10)

$$\psi^{(0)}(z, t) = \frac{\sqrt{\sigma_{z_0}}}{\left(2\pi\tilde{\sigma}_z^4(t+t_D)\right)^{1/4}} \exp\left(-\frac{(z-v_0 t)^2}{4\tilde{\sigma}_z^2(t+t_D)}\right) e^{i(p_0(z+L_D) - \varepsilon_0(t+t_D))/\hbar}, \quad (17)$$

Where $t=0$ is the entrance time of the center of the wavepacket to the interaction region at $z=0$ after a drift time t_D , $\tilde{\sigma}_z(t+t_D) = \sigma_{z_0} \sqrt{1 + i(t+t_D)/t_{R_{\parallel}}}$. The wavepacket probability distribution

$$\left|\psi^{(0)}(z, t)\right|^2 = \frac{1}{\sqrt{2\pi\sigma_z^2(t+t_D)}} \exp\left(-\frac{(z-v_0 t)^2}{2\sigma_z^2(t+t_D)}\right), \quad (18)$$

displays “particle-like” propagation at velocity $v_0 = \beta_0 c = p_0 / \gamma_0 m$ with wavepacket expansion:

$$\sigma_z(t) = |\tilde{\sigma}_z(t)| = \sigma_{z0} \sqrt{1 + t^2/t_{R_{||}}^2}. \quad (19)$$

The parameter $t_{R_{||}}$ is the evolution time from the waist for which $\sigma_z(t_{R_{||}}) = \sqrt{2}\sigma_{z0}$, in analogy to the Rayleigh length of wave diffraction. We now solve Eq.10 using the first order perturbation theory in momentum space

$$\psi(z, t) = \psi^{(0)}(z, t) + \psi^{(1)}(z, t) = \int \frac{dp}{\sqrt{2\pi\hbar}} \left(c_p^{(0)} + c_p^{(1)} \right) e^{-iE_p t/\hbar} |p\rangle. \quad (20)$$

With this substitution, integration of Eq.11 in momentum space for $c_p^{(1)}$ produces energy conserving terms of single photon emission/absorption corresponding to the two terms in the perturbation Hamiltonian (eq.10):

$$c_{p'}^{(1)(e,a)} = \frac{\pi}{2i\hbar} \int dp \langle p' | H_I^{(e,a)} | p \rangle c_p^{(0)} \delta\left(\frac{E_p - E_{p'} \mp \hbar\omega}{2\hbar}\right), \quad (21)$$

Expanding again the energy dispersion relation (eq.11) to second order, the delta function determines the quantum momentum recoil

$$p_{rec}^{(e,a)} = |p^{(e,a)} - p| = \frac{\hbar\omega}{v_0} (1 \pm \delta), \quad (22)$$

$$\delta = \frac{\hbar\omega}{2m^* v_0^2}$$

The first order perturbation momentum component is then

$$c_{p'}^{(1)(e,a)} = \frac{\pi}{iv_0} \langle p' | H_I^{(e,a)} | p \mp p_{rec}^{(e,a)} \rangle c^{(0)}(p \mp p_{rec}^{(e,a)}), \quad (23)$$

where the zero-order coefficient $c_p^{(0)}$ is given in equation (12). The matrix element is straightforwardly calculated by

$$\begin{aligned} \langle p' | H_I^{(e,a)} | p \rangle &= \int \frac{dz}{2\pi\hbar} H_I^{(e,a)}(0) e^{i(p-p')z/\hbar} \\ &= \pm \frac{ieE_0 L_I p}{4\pi\gamma_0 m \hbar \omega} \text{sinc}\left(\frac{(p - p' \mp \hbar q_z) L_I}{2\hbar}\right) e^{i(p-p' \mp \hbar q_z)z/2\hbar} e^{\pm i\phi_0}, \end{aligned} \quad (24)$$

and then simplified to

$$\langle p' | H_I^{(e,a)} | p \mp p_{rec}^{(e,a)} \rangle = \pm \left(\frac{i v_0}{\pi} \right) \Upsilon \left(\frac{p \mp p_{rec}^{(e,a)}}{p_0} \right) \text{sinc} \left(\frac{\bar{\theta}_{e,a}}{2} \right) e^{i \frac{\bar{\theta}_{e,a}}{2} \mp i \phi_0}, \quad (25)$$

and

$$c_{p'}^{(1)(e,a)} = \pm \Upsilon \left(\frac{p \mp p_{rec}^{(e,a)}}{p_0} \right) c^{(0)}(p \mp p_{rec}^{(e,a)}) \text{sinc} \left(\frac{\bar{\theta}_{e,a}}{2} \right) e^{i \frac{\bar{\theta}_{e,a}}{2} \mp i \phi_0}, \quad (26)$$

with

$$\begin{aligned} \Upsilon &= \frac{e E_0 L_I}{4 \hbar \omega}, \\ \bar{\theta}_{e,a} &= \bar{\theta} \pm \frac{\varepsilon}{2}, \end{aligned} \quad (27)$$

where $\bar{\theta} = \left(\frac{\omega}{v_0} - q_z \right) L_I$ is the classical “interaction detuning parameter”[ref.9] and

$\varepsilon = \delta \left(\frac{\omega}{v_0} \right) L_I = 2\pi \delta L_I / \beta_0 \lambda$ is the interaction–length quantum recoil parameter[ref. 13

in the context].

We now can calculate the electron momentum density distribution after interaction:

$$\begin{aligned} \rho(p') &= \rho^{(0)}(p') + \rho^{(1)}(p') + \rho^{(2)}(p') \\ &= \frac{|c^{(0)}(p')|^2 + 2 \text{Re} \{ c^{(1)*}(p') c^{(0)}(p') \} + |c^{(1)}(p')|^2}{\int dp' (|c^{(0)}(p')|^2 + |c^{(1)}(p')|^2)}, \end{aligned} \quad (28)$$

where

$$\rho^{(0)}(p') = |c^{(0)}(p')|^2 = (2\pi \sigma_{p_0}^2)^{-\frac{1}{2}} \exp \left(-\frac{(p - p_0)^2}{2\sigma_{p_0}^2} \right), \quad (29)$$

is the initial Gaussian momentum density distribution. From Eq.26, the second term (the first order in E_0) is given by

$$\rho^{(1)}(p') = \frac{2 \operatorname{Re} \left\{ c_{p'}^{(1)(e)*} c_{p'}^{(0)} + c_{p'}^{(1)(a)*} c_{p'}^{(0)} \right\}}{\int dp' \left(\left| c^{(0)}(p') \right|^2 + \left| c^{(1)}(p') \right|^2 \right)} = \frac{2Y}{1 + Y^2 \left(\operatorname{sinc} \left(\frac{\bar{\theta}_e}{2} \right) + \operatorname{sinc} \left(\frac{\bar{\theta}_a}{2} \right) \right)} \times$$

$$\operatorname{Re} \left\{ \left(\frac{p' - p_{rec}^e}{p_0} \right) \left(2\pi\sigma_{p0}^2 \right)^{-\frac{1}{2}} e^{-\frac{(p' - p_0)^2}{4\tilde{\sigma}_p^2(t_D)} - \frac{(p' - p_0 - p_{rec}^e)^2}{4\tilde{\sigma}_p^{2*}(t_D)}} \operatorname{sinc} \left(\frac{\bar{\theta}_e}{2} \right) e^{i \left(\frac{\bar{\theta}_e}{2} + \phi_0 \right)} \right.$$

$$\left. - \left(\frac{p' + p_{rec}^a}{p_0} \right) \left(2\pi\sigma_{p0}^2 \right)^{-\frac{1}{2}} e^{-\frac{(p' - p_0)^2}{4\tilde{\sigma}_p^2(t_D)} - \frac{(p' - p_0 + p_{rec}^a)^2}{4\tilde{\sigma}_p^{2*}(t_D)}} \operatorname{sinc} \left(\frac{\bar{\theta}_a}{2} \right) e^{i \left(\frac{\bar{\theta}_a}{2} - \phi_0 \right)} \right\}, \quad (30)$$

This apparently quantum regime expression depends on the quantum recoil, the synchronism condition and also the acceleration phase. For the purpose of comparison with the classical point-particle acceleration (that is maximal near synchronism - $\bar{\theta} \approx 0$), we consider the case of $\varepsilon \ll 1$ (short interaction length) and substitute $\bar{\theta}_e \approx \bar{\theta}_a \approx \bar{\theta}$. This simplifies the expression to:

$$\rho^{(1)}(p') = \frac{2\pi Y e^{-\Gamma^2/2} \operatorname{sinc} \left(\frac{\bar{\theta}}{2} \right)}{1 + 2Y^2 \operatorname{sinc}^2 \left(\frac{\bar{\theta}}{2} \right)} \cos \left(\frac{\bar{\theta}}{2} + \phi_0 + \varphi \right) \left| C_{p'}^{(0)} \right|^2$$

$$\left((p' - p_{rec}^e) e^{-\left(\frac{p' - p_0}{2\sigma_{p0}^2} \right) p_{rec}^e + \delta^2} - (p' + p_{rec}^a) e^{-\left(\frac{p' - p_0}{2\sigma_{p0}^2} \right) p_{rec}^a - \delta^2} \right), \quad (31)$$

where

$$\varphi = \frac{2\omega t_D}{mv_0} (p' - p_0),$$

$$\Gamma = \frac{\omega}{v_0} \sigma_z(t_D) = \frac{2\pi\sigma_z(t_D)}{\beta\lambda}. \quad (32)$$

The decay coefficient $e^{-\Gamma^2/2}$ assures that the first order term of the momentum distribution $\rho^{(1)}$ is diminished when $\Gamma \gg 1$, namely when the wavepacket expands on its way from the source beyond the size of the interaction wavelength. Eq.31 can be further simplified by first order expansion in $\delta \ll 1$, resulting in

$$\rho^{(1)}(p') = 4 \left(\frac{\hbar\omega/v_0}{p_0} \right) \Upsilon \rho^{(0)}(p') \text{sinc} \left(\frac{\bar{\theta}}{2} \right) e^{-\Gamma^2/2} \cos \left(\frac{\bar{\theta}}{2} + \phi_0 + \varphi \right) \left[1 + \frac{\Gamma^2 p'}{2m^* v_0} - \frac{(p' - p_0) p'}{2\sigma_{p_0}^2} \right]. \quad (33)$$

The third term in Eq.28 (second order in E_0) is proportional to $\left| c_{p'}^{(1)(e)} + c_{p'}^{(1)(a)} \right|^2$. In the present context we are interested in the PINEM case where $p_{rec}^{(0)} = \frac{\hbar\omega}{v_0} > \sigma_{p_0}$. In this case we neglect the interference terms of the emission and absorption side bands and obtain:

$$\rho^{(2)}(p') \simeq \left(\left| c^{(1)(e)}(p') \right|^2 + \left| c^{(1)(a)}(p') \right|^2 \right) - \rho^{(0)}(p') \int dp' \left(\left| c^{(1)(e)}(p') \right|^2 + \left| c^{(1)(a)}(p') \right|^2 \right) \quad (34)$$

To second order in terms of $\Upsilon < 1$, one obtains

$$\begin{aligned} \rho^{(2)}(p') = & \Upsilon^2 \left[\left(\frac{p' + p_{rec}^e}{p_0} \right)^2 \rho^{(0)}(p' + p_{rec}^e) - \rho^{(0)}(p') \right] \text{sinc}^2 \left(\frac{\bar{\theta}_e}{2} \right) \\ & + \Upsilon^2 \left[\left(\frac{p' - p_{rec}^a}{p_0} \right)^2 \rho^{(0)}(p' - p_{rec}^a) - \rho^{(0)}(p') \right] \text{sinc}^2 \left(\frac{\bar{\theta}_a}{2} \right). \end{aligned} \quad (35)$$

3. Measurement limits

It is necessary to realize that conventional electron energy spectroscopy necessitates averaged measurement of a multitude of electrons, in order to view the momentum distribution. The momentum distribution of an ensemble of electrons is found from spatial (z) coordinate integration of the Wigner distribution in p-z phase-space for fixed p [1] (See Fig. 2). For an ensemble of uncorelated single electron measurements this reduces to a simple classical statistical averaging integral of the initial (thermal) central momenta distribution with the single electron wavepacket momentum distributions:

$$\rho_{en} = \int \rho^{(0)}(p', p_0) f\left(\frac{p_0 - P_{0,en}}{\sigma_{p,th}}\right) dp_0, \quad (36)$$

This, necessarily, results in widening of the measurable standard deviation of the Gaussian distribution of the ensemble to $\sigma_{p,en}$:

$$\sigma_{p,en}^2 = \sigma_{p,th}^2 + \sigma_{p_0}^2. \quad (37)$$

Since the measurable distribution satisfies $\sigma_{p,en} > \sigma_{p_0}$, the wavepacket broadening cannot be distinguished from the thermal distribution that determines the so called “Coherence time” of electron microscopes $t_{coh} = \hbar / 2\sigma_{E,en}$ (typically $\sigma_{E,en} < 0.7\text{eV}$). However, the quantum recoil effect on the momentum distribution of both emission and absorption is still observable if $p_{rec}^{(0)} > \sigma_{p,en}$ as shown in Figure 2 in agreement with PINEM experiments[ref:18-22 in the text].

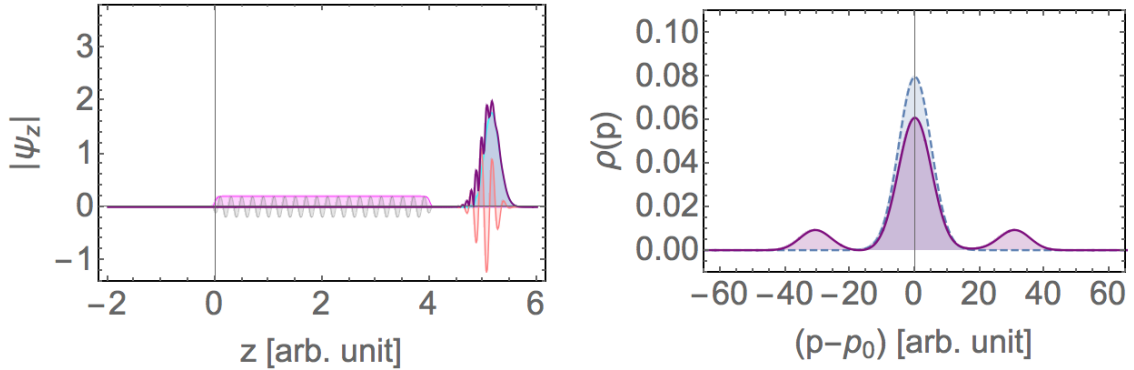
One may want to use momentum distribution measurement after electron radiative interaction in the phase-dependent wavepacket regime, in order to determine the quantum-wavepacket dimensions of electrons emitted from natural electron emission sources. But measurement of the electron momentum distribution requires normally accumulation of data from an ensemble of particles emitted from the electron source. Measurements of the wavepacket characteristics of electrons, photo-emitted from single-electron emission sources like a tip [2] or an ion cold-trap [3], would be

usually masked by random (thermal) spread of the particles in the ensemble (Eq.36). Because of the ensemble random (thermal) momentum spread, after a short drift length, the classical statistical spatial spread of the ensemble exceeds the size of the individual wavepackets [4]. This limits the practical range within which the stimulated interaction experiment can be carried out, unless the electron beam source is very cold and a protected weak measurements of Aharonov-Vaidman's kind [5] could be employed.

4. Numerical simulation

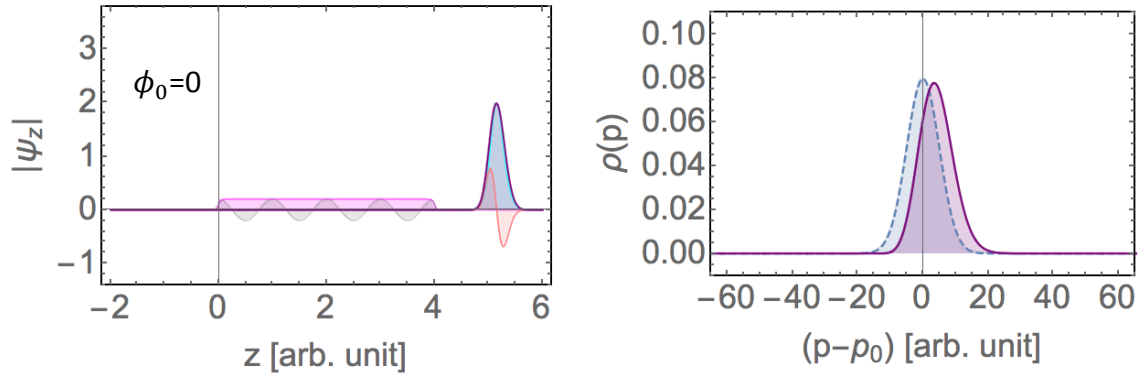
Video-1: Simulation of stimulated interaction in the quantum large recoil limit.

Wavepacket evolution for the case $\bar{\theta}=0$ and weak field $\Upsilon \ll 1, \sigma_{p_0} < \hbar\omega/v_0, \sigma_z(t_D) > \lambda\beta_0$, with sidebands formation and no net acceleration: simulation parameters $\beta_0=0.7$, $2\sigma_{z_0}/\beta_0\lambda=1$, $\Upsilon=0.2$, $\phi_0=0$

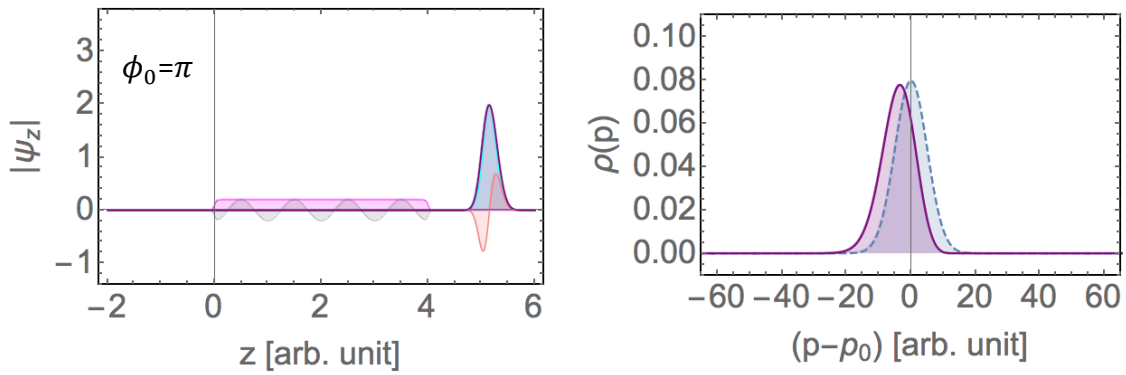


(Left) Evolution in space $-z$ (pink- $\text{Im}\Psi(z)$, cyan- $\text{Re}\Psi(z)$ and purple- $|\Psi(z)|$), the central pink area is the near-field radiation amplitude and phase. (Right) Evolution in momentum $\rho(p) = |\Psi(p)|^2$ is symmetric without net momentum gain.

Video-2: Simulation of phase-dependent stimulated interaction in the the wavepacket near “point-particle” limit. Wavepacket evolution for the case $\bar{\theta}=0$ and weak field $\Upsilon \ll 1, \sigma_z(t_D) < \lambda\beta_0$, with simulation parameters: $\beta_0 = 0.7$, $2\sigma_{z_0}/\beta_0\lambda = 0.2$, $\Upsilon = 0.2$. (a) $\phi_0 = 0$ (acceleration); (b) $\phi_0 = \pi$ (decceleration):

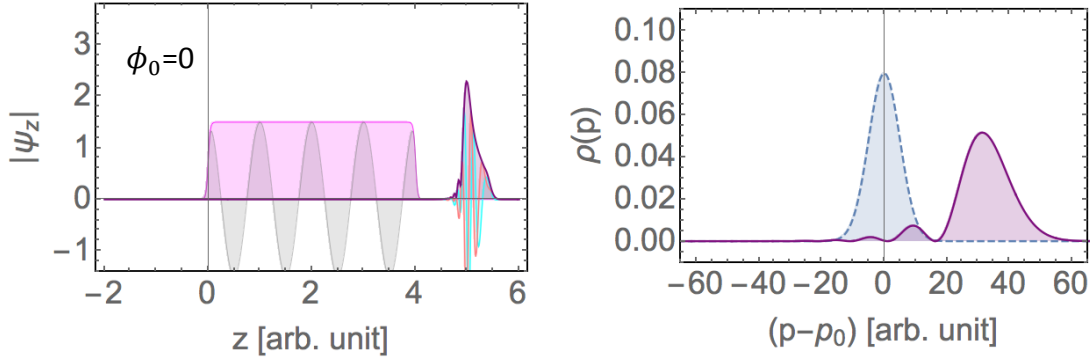


- a. (Left) Evolution in space- z . (Right) Evolution in momentum $\rho(p) = |c(p)|^2$ with net momentum gain.

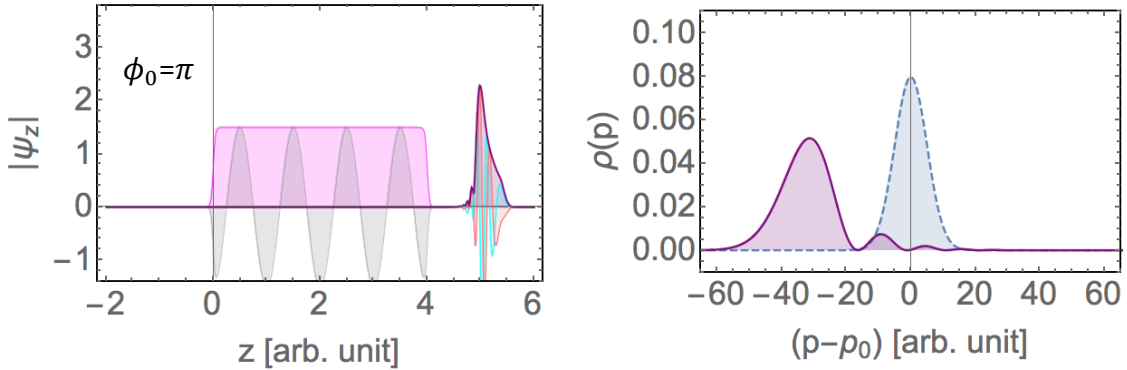


- b. (Left) Evolution in space- z . (Right) Evolution in momentum $\rho(p) = |c(p)|^2$ with net negative momentum gain.

Video-3: Simulation of phase-dependent interaction in the near “point-particle” limit. Wavepacket evolution for the case $\bar{\theta}=0$ and strong field (multiphoton exchange) $\Upsilon > 1, \sigma_z(t_D) < \lambda\beta_0$ with simulation parameters: $\beta_0 = 0.7$, $2\sigma_{z_0}/\beta_0\lambda = 0.2$, $\Upsilon = 1.5$. (a) $\phi_0 = 0$ (acceleration); (b) $\phi_0 = \pi$ (decceleration):



a. (Left) Evolution in space- z . (Right) Evolution in momentum $\rho(p) = |c(p)|^2$ with net momentum gain.



b. (Left) Evolution in space- z . (Right) Evolution in momentum $\rho(p) = |c(p)|^2$ with net negative momentum gain.

REFERENCES

33. W. P. Schleich "Quantum Optics in Phase Space", John Wiley & Sons, 2011.
34. Michael Kruger, Markus Schenk, Peter Hommelhoff, *Nature* **475**: 78 -81 (2011).
35. W.J. Engelen, E.J.D. Vredenburg, O.J. Luiten, *Ultramicroscopy* **147**, 61–69 (2014).
36. Ford, G. W., and R. F. O'connell. *American Journal of Physics* **70.3**: 319-324(2002).
37. Aharonov, Yakir, and Lev Vaidman. "The two-state vector formalism: an updated review." In *Time in quantum mechanics*, 399-447. Springer Berlin Heidelberg (2008).